Optics Letters

Spectral correlation and interference in non-degenerate photon pairs at telecom wavelengths

Paulina S. Kuo,[1,*] Thomas Gerrits,[2] Varun B. Verma,[2] and Sae Woo Nam[2]

[1]Information Technology Laboratory, National Institute of Standards and Technology, 100 Bureau Drive, Gaithersburg, Maryland 20899, USA
[2]Physical Measurement Laboratory, National Institute of Standards and Technology, 325 Broadway, Boulder, Colorado 80305, USA
*Corresponding author: paulina.kuo@nist.gov

Received 24 August 2016; revised 28 September 2016; accepted 6 October 2016; posted 7 October 2016 (Doc. ID 272564); published 31 October 2016

We characterize an entangled-photon-pair source that produces signal and idler photons at 1533 nm and 1567 nm using fiber-assisted signal-photon spectroscopy. By erasing the polarization distinguishability, we observe interference between the two down-conversion paths. The observed interference signature is closely related to the spectral correlations between photons in a Hong–Ou–Mandel interferometer. These measurements suggest good indistinguishability between the two down-conversion paths, which is required for high entanglement visibility.

OCIS codes: (270.5585) Quantum information and processing; (190.4410) Nonlinear optics, parametric processes.

http://dx.doi.org/10.1364/OL.41.005074

Entangled photon pairs are key components in quantum information processing. They are used in many quantum information applications including quantum key distribution [1], connecting quantum nodes [2], tests of the Bell inequality [3–6], and generation of certified random numbers [7]. One of the most common ways to produce entangled photon pairs is by spontaneous parametric down-conversion (SPDC), where a short-wavelength pump photon is split into a signal and idler photon pair. Indistinguishability of certain degrees of freedom of the down-converted photons is a key requirement for high-quality entanglement since distinguishing information (such as wavelength, arrival time, or direction of travel) can destroy the interference effects that are a fundamental part of entanglement experiments [8,9]. However, it is possible to design an entangled-photon-pair source with unequal or non-degenerate signal and idler wavelengths. In these sources, interference occurs between photons generated in two down-conversion paths, such as two paths in an interferometer [10–12] or two separate nonlinear crystals [13,14].

A common method for measuring photon distinguishability is to use a Hong–Ou–Mandel (HOM) interferometer [15]. Recently, spectrally resolved studies of HOM interference have been performed [16], which give additional insights into the origins of the indistinguishability. The spectral dependence of correlations is obtained using fiber-assisted single-photon spectroscopy [16–19]. This spectroscopy technique is fast and powerful. It translates the fine temporal resolution of photodetectors such as superconducting nanowire single-photon detectors (SNSPDs) into fine spectral resolution by sending the spectrum under test through a dispersive delay line, typically a long section of optical fiber. Single-photon-level spectra can be acquired quickly using time-correlated single-photon-counting electronics. Post-processing allows observation of spectrally resolved photon correlations.

We apply fiber-assisted single-photon spectroscopy to a photon-pair source based on SPDC using a continuous-wave (CW) pump laser. This source is designed to produce signal (s) and idler (i) photons at 1533 nm and 1567 nm, respectively. We use periodically poled $LiNbO_3$ (PPLN) with an aperiodic domain structure [20–22] designed to simultaneously phase match $|H_s\rangle|V_i\rangle$ and $|V_s\rangle|H_i\rangle$ [23,24], where H and V represent horizontally and vertically polarized photons, respectively. The observed single-photon spectra agree well with theoretical calculations. We explore the distinguishability of the two parallel down-conversion processes through these measurements. We observe an interference feature that we identify as interference between the two possible down-conversion paths.

In this Letter, we present our results toward the development of a polarization-entangled photon-pair source in the telecommunications wavelength range based on a quasi-phase-matched (QPM) crystal. Polarization-entangled SPDC sources have been produced using two consecutive co-rotated crystals [13,14] or by using two consecutive QPM periods [25,26]. More recently, an interlaced, bi-periodic structure has been used [27]. The source used in this work is based on an aperiodically poled $LiNbO_3$ bulk crystal (details are described in [24]). The domain structure is similar to the structure proposed theoretically in [28]. The $LiNbO_3$ crystal was 25 mm in length. We confocally focused a CW 775 nm wavelength pump to a 40 μm waist inside the crystal. After rejecting the pump with a dichroic filter at near-normal incidence, the signal and idler photons are sent to a half-wave plate (HWP) and a polarizing beam splitter (PBS). The HWP is set to either rotate all polarizations by 45° or to have no effect. One output of the PBS is sent through a dispersion compensation module (DCM) that

spreads the spectral components by approximately −1 ns/nm (the negative sign indicates that the longer wavelengths lead the shorter wavelengths). The SNSPDs have a roughly 100 ps timing jitter, which when combined with the −1 ns/nm dispersion implies 0.1 nm spectral resolution of the measurement. The DCM has a 4 dB insertion loss and produces 30 μs of fixed delay. Both outputs of the PBS go to SNSPDs and time-tagging electronics that record the relative start and stop times. A sketch of the experimental setup is shown in Fig. 1. The wavelength axis of the measured spectra corresponds to the wavelength of photons in the dispersed port of the PBS. In Fig. 1, these are the photons that arrive at detector 1 (D1).

In contrast to pulsed SPDC sources that use the pump pulses as a trigger for the timing electronics in fiber-assisted single-photon spectroscopy, we use the fact that the pump is narrowband, which means there is a one-to-one correspondence in wavelength between the down-converted signal and its matching idler photon. Therefore, the relative arrival time between the signal and idler photons uniquely determines the wavelengths of both photons. Using a calibration of the DCM delay as a function of wavelength, we constructed a lookup table between signal-idler arrival time and wavelength.

Figure 2(a) shows the SPDC spectra measured using the fiber-assisted spectroscopy technique. The HWP is not used in these spectrograms. The x-axis is the wavelength associated with the dispersed photons that arrive at D1—in this case, the horizontally polarized photons. The wavelengths of the corresponding vertically polarized photons can be calculated using energy conservation. The H photons tune to longer wavelengths with increasing temperature, while the V photons tune to shorter wavelengths. At $T = 143$°C, the wavelengths of the H and V polarized photons become equal, $\lambda(H_s) = \lambda(V_s)$ and $\lambda(H_i) = \lambda(V_i)$. These spectra agree with previously measured spectra based on difference frequency generation [23].

The half-wave plate has several interesting effects on the experiment. When the HWP is set to rotate all polarizations by 45°, it removes the polarization selectivity of the polarizing beam splitter. For the fiber-assisted spectrogram measurement, the effect of the HWP is to send both H- and V-polarized photons to both arms. This causes both H-polarized and V-polarized photon peaks to register in the spectrogram, as illustrated in Fig. 2(b). Observation of the four peaks allows the fixed time delay between the two arms to be detected with high accuracy. This time delay is the reference delay that, when combined with the wavelength calibration, allows proper matching of both pairs of H- and V-polarized peaks. As a result, a careful characterization of the fixed delay difference between the two arms is not necessary.

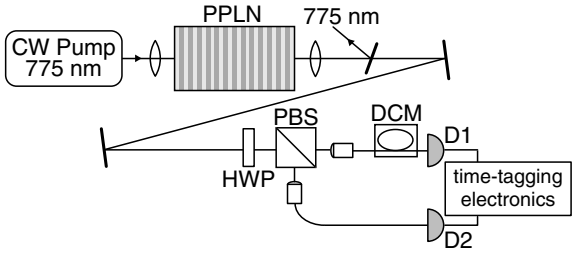

Fig. 1. Diagram of experimental setup. HWP, half-wave plate; PBS, polarizing beam splitter; DCM, dispersion compensation module; D1(2), detector 1(2).

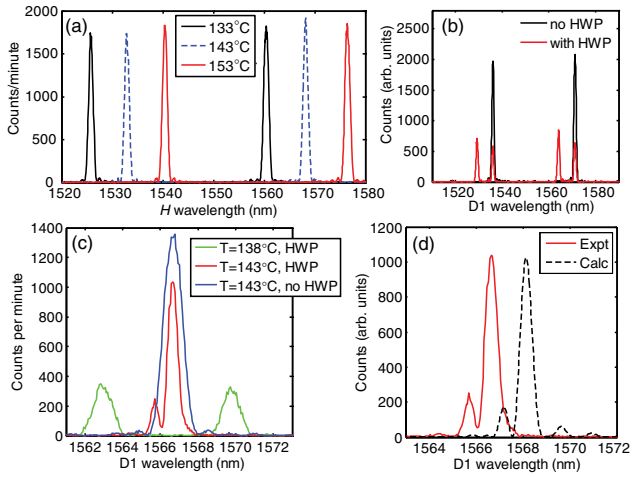

Fig. 2. (a) Single-photon SPDC spectrogram measured at different crystal temperatures. Peaks near 1530 nm correspond to the $|H_s\rangle|V_i\rangle$ process, while peaks near 1570 nm are the $|V_s\rangle|H_i\rangle$ process. (b) Inserting the HWP to erase polarization selectivity of the PBS causes both H- and V-polarized peaks to appear in the spectrogram. (c) Temperature tuning to $T = 143$°C (where wavelengths are equal) reveals interference in the spectrogram. Interference disappears when the HWP is removed. (d) Comparison of theoretical interference spectrogram (dashed) to experiment (solid). The small offset in the center wavelength can be attributed to uncertainty in the dispersion relation.

When the HWP erases the polarization distinguishability of the PBS, the spectrograms reveal an interference signature that is related to interference between the two down-conversion paths. With the HWP present and the PPLN temperature at 138°C where $\lambda(H_i) \neq \lambda(V_i)$, two separate peaks are visible in the spectrogram near 1565 nm [green trace of Fig. 2(c)]. When the crystal temperature is raised to 143°C, the wavelengths of the two peaks overlap and we see interference. However, when the HWP is removed, the interference disappears. There is a clear difference in the shape of the spectrograms caused by the presence or absence of the HWP.

The sketch in Fig. 3 illustrates the critical role of the HWP for interference. Without the HWP rotating the polarizations by 45°, the two down-conversion paths ($|H_s\rangle|V_i\rangle$ or $|V_s\rangle|H_i\rangle$) are distinguishable after separation by the PBS. The paths are distinguishable in the sense that the wavelength of the photon arriving at one detector immediately reveals which path was taken. When the HWP rotates the polarizations and removes the polarization distinguishability of the PBS, this distinguishability is erased and interference becomes possible. The HWP enables the interference between the two down-conversion paths.

The interference fringes can be understood in terms of spectrally resolved HOM interference. The joint spectral intensity (JSI) distribution of two photons exiting opposite ports of a beam splitter is given by [16,29]

$$I(\omega_1,\omega_2) \propto \frac{1}{2}|C(\omega_1,\omega_2)e^{i(\omega_1 t_1+\omega_2 t_2)} - C(\omega_2,\omega_1)e^{i(\omega_2 t_1+\omega_1 t_2)}|^2, \quad (1)$$

where $C(\omega_1,\omega_2)$ is the joint spectral amplitude of the two-photon wave-function incident on the beam splitter, ω_1 and

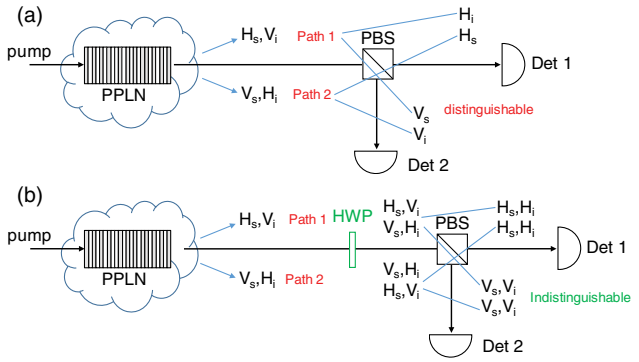

Fig. 3. (a) Without the HWP, the paths are distinguishable since the wavelengths of the signal and idler are different. (b) With the HWP (which causes H- and V-polarizations to be sent to both arms), the paths are indistinguishable.

ω_2 refer to the frequencies of the two photons, and t_1 and t_2 are their corresponding arrival times. When $\Delta t = t_1 - t_2 = 0$, the HOM interference dip is obtained if

$$C(\omega_1, \omega_2) = C(\omega_2, \omega_1). \quad \textbf{(2)}$$

If the SPDC is degenerate, then Eq. (2) is satisfied since $\omega_1 = \omega_2$. However, non-degenerate SPDC sources can show HOM interference if the joint spectral amplitude is engineered to satisfy Eq. (2). This requirement is identical to the stipulation that the joint spectral amplitude $C(\omega_1, \omega_2)$ be symmetric about the line $\omega_1 = \omega_2$ when plotted in the $\omega_1 - \omega_2$ plane [29]. Our SPDC source achieves this symmetry at a crystal temperature of 143°C. Figure 4(a) shows the JSI distribution of the source, $|C(\omega_1, \omega_2)|^2$, for the process near 1532 nm, 1568 nm. This distribution is the narrowband pump multiplied by the sinc^2 phase-matching function. The nonlinear crystal is approximated by two QPM periods that phase match $|H_s\rangle|V_i\rangle$ and $|V_s\rangle|H_i\rangle$. The CW pump laser is modeled as having 0.3 pm bandwidth.

Equation (1) shows that interference fringes are present all along the HOM interference dip [16]. That is, if one calculates $I(\omega_1, \omega_2)$ for different Δt, oscillations are present in the JSI distribution for $\Delta t \neq 0$. The spectral fringes increase in frequency with larger Δt. In our experiment, the signal and idler arrive at the beam splitter at unequal times because of temporal walk-off due to birefringence in the PPLN crystal. For $LiNbO_3$, the index difference at 1550 nm is $\Delta n = 0.0732$ [30] so that $\Delta t = \Delta n L/2c = 3$ ps. As a comparison, the width of the HOM dip is given by the coherence time of the photon packet [15]. From spectral measurements, the bandwidth of the down-conversion is $\Delta f = 4.2\ \text{cm}^{-1}$ for $\Delta\lambda = 1$ nm so that the coherence time [31] is $\sqrt{(2\ln 2)/\pi}/\Delta f = 5.3$ ps. Thus the measurements taken here occur on the shoulder of the HOM dip.

We can use Eq. (1) together with $LiNbO_3$ dispersion data [30] to calculate the expected JSI distribution for HOM interference. Figure 4(b) shows the calculated spectral correlations near the HOM dip with $\Delta t = 3$ ps. Projecting this theoretical distribution on the vertical axis gives the calculated spectrum shown in Fig. 2(d), which is in good agreement with the experimental interference spectrum. Note that the resolution of our spectrometer (0.1 nm) limits the visibility of the

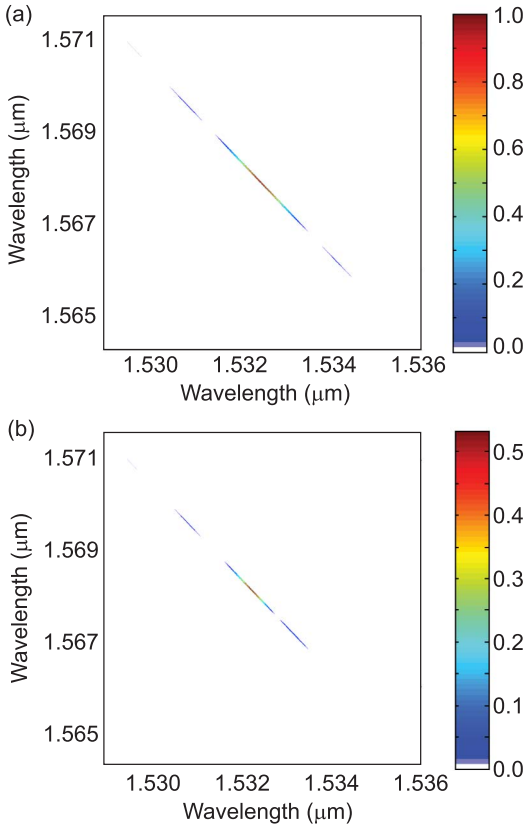

Fig. 4. Theoretical (a) joint spectral distribution of the source, $|C(\omega_1, \omega_2)|^2$ and (b) joint spectral intensity distribution after HOM interference calculated from Eq. (1) using $\Delta t = 3$ ps. The plots show the joint spectrum of the process near (1532 nm, 1568 nm), while the other process (not shown) is at (1568 nm, 1532 nm). There is slight asymmetry in the JSI after interference compared to $|C(\omega_1, \omega_2)|^2$ shown in (a).

experimental fringe. There is also a slight offset between the center wavelength of the calculated and measured spectra, which is likely due to uncertainty in the dispersion function.

Photon-pair sources with unequal signal and idler wavelengths show interference, and this interference can be understood only by considering the total biphoton wave packet. It is clear from the sketch in Fig. 3 that the interference is not between individual photons but between the different paths. Each of the two paths contains pairs of photons with non-degenerate wavelengths. The wavelengths of the photons in one path must match the wavelengths in the other path, otherwise there is distinguishing information and there is no interference [see the green trace in Fig. 2(c), for instance]. It is this path interference that allows entanglement using non-degenerate signal and idler wavelengths.

We believe that this measurement is a useful part of a full characterization of the polarization-entangled photon-pair source. The clear interference signature suggests that the source has good indistinguishability between the two simultaneous down-conversion processes. The next step will be to measure the polarization correlations [3]. The interference fringes observed through spectrally resolved HOM interference suggest that once temporal distinguishability is removed by temporal compensation, the source will have good polarization

entanglement performance. In fact, the spectrally resolved HOM measurement could be a useful tool in diagnosing sources of distinguishability that lead to poor polarization correlations.

In conclusion, we have developed a dual-process SPDC crystal based on PPLN and we characterized the parametric down-conversion using fiber-assisted single-photon spectroscopy. We have used this technique to perform spectrally resolved HOM interference. We observed interference between the two down-conversion paths and show how this interference depends on erasing the polarization distinguishability. A theoretical model for the interference is presented, which shows excellent agreement with the experimental spectrogram. Observation of the interference is complementary to the measurement of polarization correlation, and it is a useful stepping stone toward demonstrating the utility of this source for entangled-photon-pair generation.

Acknowledgment. The authors would like to thank O. Slattery for assistance with equipment.

REFERENCES

1. C. H. Bennett and G. Brassard, in *Proceedings of IEEE International Conference on Computers, Systems and Signal Processing* (1984), pp. 175–179.
2. H. J. Kimble, Nature **453**, 1023 (2008).
3. Y. H. Shih and C. O. Alley, Phys. Rev. Lett. **61**, 2921 (1988).
4. P. G. Kwiat, K. Mattle, H. Weinfurter, A. Zeilinger, A. V. Sergienko, and Y. Shih, Phys. Rev. Lett. **75**, 4337 (1995).
5. L. K. Shalm, E. Meyer-Scott, B. G. Christensen, P. Bierhorst, M. A. Wayne, M. J. Stevens, T. Gerrits, S. Glancy, D. R. Hamel, M. S. Allman, K. J. Coakley, S. D. Dyer, C. Hodge, A. E. Lita, V. B. Verma, C. Lambrocco, E. Tortorici, A. L. Migdall, Y. Zhang, D. R. Kumor, W. H. Farr, F. Marsili, M. D. Shaw, J. A. Stern, C. Abellán, W. Amaya, V. Pruneri, T. Jennewein, M. W. Mitchell, P. G. Kwiat, J. C. Bienfang, R. P. Mirin, E. Knill, and S. W. Nam, Phys. Rev. Lett. **115**, 250402 (2015).
6. M. Giustina, M. A. M. Versteegh, S. Wengerowsky, J. Handsteiner, A. Hochrainer, K. Phelan, F. Steinlechner, J. Kofler, J.-A. Larsson, C. Abellán, W. Amaya, V. Pruneri, M. W. Mitchell, J. Beyer, T. Gerrits, A. E. Lita, L. K. Shalm, S. W. Nam, T. Scheidl, R. Ursin, B. Wittmann, and A. Zeilinger, Phys. Rev. Lett. **115**, 250401 (2015).
7. S. Pironio, A. Acin, S. Massar, A. B. de la Giroday, D. N. Matsukevich, P. Maunz, S. Olmschenk, D. Hayes, L. Luo, T. A. Manning, and C. Monroe, Nature **464**, 1021 (2010).
8. Y. Shih, IEEE J. Sel. Top. Quantum Electron. **9**, 1455 (2003).
9. W. P. Grice, A. B. U'Ren, and I. A. Walmsley, Phys. Rev. A **64**, 063815 (2001).
10. M. Fiorentino, G. Messin, C. E. Kuklewicz, F. N. C. Wong, and J. H. Shapiro, Phys. Rev. A **69**, 041801 (2004).
11. T. Kim, M. Fiorentino, and F. N. C. Wong, Phys. Rev. A **73**, 012316 (2006).
12. P. G. Evans, R. S. Bennink, W. P. Grice, T. S. Humble, and J. Schaake, Phys. Rev. Lett. **105**, 253601 (2010).
13. P. G. Kwiat, E. Waks, A. G. White, I. Appelbaum, and P. H. Eberhard, Phys. Rev. A **60**, R773 (1999).
14. M. Pelton, P. Marsden, D. Ljunggren, M. Tengner, A. Karlsson, A. Fragemann, C. Canalias, and F. Laurell, Opt. Express **12**, 3573 (2004).
15. C. K. Hong, Z. Y. Ou, and L. Mandel, Phys. Rev. Lett. **59**, 2044 (1987).
16. T. Gerrits, F. Marsili, V. B. Verma, L. K. Shalm, M. Shaw, R. P. Mirin, and S. W. Nam, Phys. Rev. A **91**, 013830 (2015).
17. W. B. Whitten and H. H. Ross, Anal. Chem. **51**, 417 (1979).
18. M. Avenhaus, A. Eckstein, P. J. Mosley, and C. Silberhorn, Opt. Lett. **34**, 2873 (2009).
19. T. Gerrits, M. J. Stevens, B. Baek, B. Calkins, A. Lita, S. Glancy, E. Knill, S. W. Nam, R. P. Mirin, R. H. Hadfield, R. S. Bennink, W. P. Grice, S. Dorenbos, T. Zijlstra, T. Klapwijk, and V. Zwiller, Opt. Express **19**, 24434 (2011).
20. M. Asobe, O. Tadanaga, H. Miyazawa, Y. Nishida, and H. Suzuki, Opt. Lett. **28**, 558 (2003).
21. M. Asobe, O. Tadanaga, H. Miyazawa, Y. Nishida, and H. Suzuki, IEEE J. Quantum Electron. **41**, 1540 (2005).
22. J. S. Pelc, P. S. Kuo, O. Slattery, L. Ma, X. Tang, and M. M. Fejer, Opt. Express **20**, 19075 (2012).
23. P. S. Kuo, J. S. Pelc, O. Slattery, L. Ma, and X. Tang, Proc. SPIE **9136**, 913603 (2014).
24. P. S. Kuo, T. Gerrits, V. Verma, S. W. Nam, O. Slattery, L. Ma, and X. Tang, Proc. SPIE **9762**, 976211 (2016).
25. T. Suhara, G. Nakaya, J. Kawashima, and M. Fujimura, IEEE Photon. Technol. Lett. **21**, 1096 (2009).
26. W. Ueno, F. Kaneda, H. Suzuki, S. Nagano, A. Syouji, R. Shimizu, K. Suizu, and K. Edamatsu, Opt. Express **20**, 5508 (2012).
27. H. Herrmann, X. Yang, A. Thomas, A. Poppe, W. Sohler, and C. Silberhorn, Opt. Express **21**, 27981 (2013).
28. K. Thyagarajan, J. Lugani, S. Ghosh, K. Sinha, A. Martin, D. B. Ostrowsky, O. Alibart, and S. Tanzilli, Phys. Rev. A **80**, 052321 (2009).
29. K. Wang, J. Phys. B **39**, R293 (2006).
30. G. J. Edwards and M. Lawrence, Opt. Quantum Electron. **16**, 373 (1984).
31. M. Fox, *Quantum Optics: An Introduction* (Oxford University, 2006).